Surface Segregated Layer and Native Oxide Layer Formed on High-Purity Iron Base Alloys by Angle-Resolved XPS

Shigeru Suzuki

Institute for Advanced Materials Processing, Tohoku University
Katahira, Sendai 980-77, Japan

ABSTRACT

An attempt has been made to describe recent views on segregated layers and native oxide layers formed on the surface of high-purity iron based alloys by applying angle-resolved x-ray photoelectron spectroscopy (AR-XPS). It is worth mentioning that AR-XPS is suitable for characterizing thin surface layers non-destructively, since their thickness is nanometer order of magnitude, being comparable to inelastic mean free paths of X-ray photoelectrons. This overview focuses the results on surface segregated layers of alloying and impurity elements such as chromium, phosphorus and sulfur in those alloys. It is also indicated that the amount of surface segregated chromium considerably affects formation of a native oxide layer in iron base alloys.

1. INTRODUCTION

Characterization of very thin layers at the surface and interface in iron and steel is known to play an important role in controlling their processes and improving their properties. Then, microscopic characterization becomes indispensable for developing high-quality iron base alloys, although they are considered typical conventional materials.

There are two important surface phenomena occurring in surface layers of atomic scale thickness on metallic materials. One is surface segregation of a constituent element, which is enrichment of an alloying or impurity element to the specimen surface induced by heating under vacuum. Typically, surface segregation were investigated for iron - non-metallic element systems (for example, Fe-C /1-3/, Fe- N /3,4/, Fe-Si /5-9/, Fe-P /10/, Fe-Sn /11-15/, Fe-Sb /16-18/) and iron - metallic element systems (for example, Fe-Ti /19/, Fe-Cr /19-29/, Fe-Mo /19/). In these experiments, some interesting results were obtained by finding systematic compositional change on the specimen surface. However, the amount of surface segregation for an element seemed to be often affected by other coexisting impurities, since the amount and state of impurities in iron or steel specimens used were not enough controlled. Therefore, in order to understand intrinsic surface behaviors of each element, investigations are strongly required with respect to surface segregation in well-controlled specimens.

Another important phenomenon occurring on the specimen surface is formation of a native oxide, which takes place when the specimen surface is exposed to air or a low partial pressure of oxygen at about room temperature. Thickness of native oxide layers in iron and steel is also nanometer order of magnitude /30-37/, and they are considered to affect their weathering, corrosion and so on. Nevertheless, thickness values of native oxide layers and the influence of the surface composition on the oxide layers have not yet been systematically characterized.

Surface-analytical methods such as Auger electron spectroscopy (AES), X-ray photoelectron spectroscopy (XPS) have often been applied to characterization of the surface layers of iron base alloys. Furthermore, XPS and AES depth profiling, which is combination XPS and AES measurements and ion sputtering, are often performed for obtaining information of the surface layers. However, clear depth profiles are hardly determined by these XPS or AES depth profiling, as exemplified in Fig.1, where an XPS depth profile is illustrated using the results of Fe-25%Cr alloy exposed to air after chromium segregation. In this paper, unit of the bulk concentration is expressed as %, that is mass%, and the surface concentration is at% or atomic fraction.

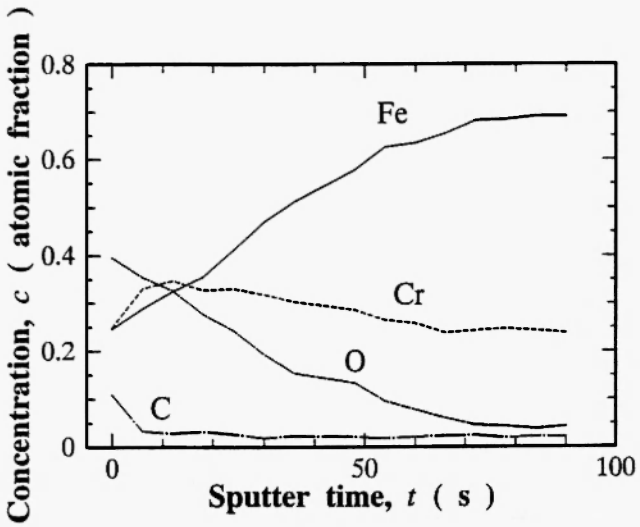

Fig.1: Depth profile of Fe-25%Cr exposed to air after chromium segregation.

Although slight enrichment of chromium on the specimen surface is observed in the depth profile of Fe-25%Cr alloy, it may not always give the real surface structure. This is based on reason that thickness of such surface layer is comparable to the escape depth of photoelectrons, which means that XPS spectra contain signals from not only the surface but also the substrate. It should also be noted that atomic mixing of constituent elements may be accompanied with ion sputtering on the specimen surface.

Contrary to depth profiling with ion sputtering, angle resolved XPS (AR-XPS) appears to be effective for characterizing very thin layers formed on the specimen surface /38/. AR-XPS, in which photo-electrons are measured by changing the take-off angle against the specimen surface, has sometimes been applied for characterization of surface layers /36,37/, and their advantages clearly encourage further application to surface analysis of materials.

With this background in mind, AR-XPS studies were systematically made for characterizing the surface segregated layers and native oxide layers formed on the surface of high-purity base iron alloys /39-45/. Surface behaviors of high-purity iron and its base alloys are also subject for their excellent surface properties /46,47/. This overview covers the recent AR-XPS experimental results surface segregation of several alloying and impurity elements, such as chromium, phosphorus and sulfur on the iron surface of high-purity base and the effect of the surface segregation, particularly chromium, on the native oxide layer formed on the surface of these alloys.

2.EXPERIMENTAL

2.1.Specimens

Plates of high-purity iron base alloys, which were produced by special methods /44-47/, were prepared. They were annealed at high temperatures and polished with emery papers and buffing using alumina powder. They were finally washed with acetone before being introduced into an ultra vacuum chamber attached to a XPS spectrometer. The specimens were polycrystalline, and the grain size was between 30 and 100 micronmeter.

The specimens were cleaned by argon ion sputtering operated at 3 kV in an XPS spectrometer under ultra high vacuum, in order to obtain a contamination-free surface. The surface with segregation of alloying or impurity elements was mainly obtained by *in-situ* heating at 973 K for 300 s under ultra high vacuum (10^{-8} Pa) after argon sputtering. The amount of a surface segregated element, which is in equilibrium with the bulk amount, depends on heating temperature, and it provides free energy for surface segregation /48/. However, since it takes a prolonged time to reach equilibrium at lower temperatures, a temperature at about 1000K was chosen for equilibrium segregation in this work. Native oxide layers on the specimen surface were typically formed by exposing the specimens to air at 298 K, since native oxide thickness for iron is known to be almost independent of the exposure time.

2.2 Measurements

Measurements of XPS were given in detail in previous works /39-45/. Only some essential points are given below. An XPS apparatus with a computer aided tilting stage was used, and the incident X-ray was monochromated Al Kα radiation. The take-off angle, corresponding to the angle between the direction of an analyzer and the specimen plane, was changed from 15 degrees to 75 degrees in the AR-XPS measurements.

As a typical example, Figure 2 shows the

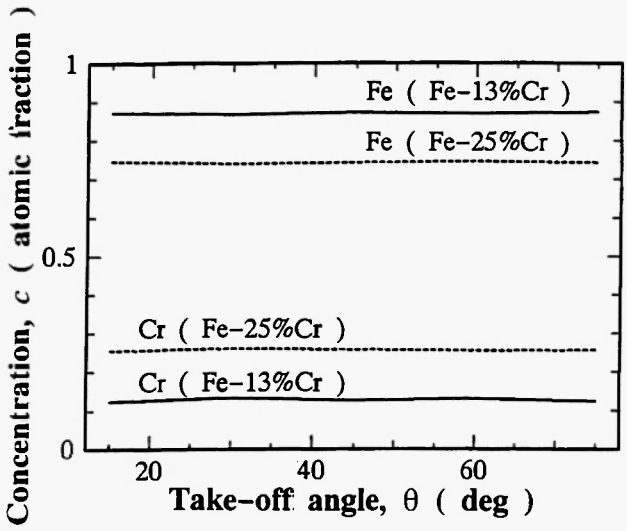

Fig.2: The concentration of iron and chromium versus take-off angle for the sputter cleaned Fe - 13% Cr and Fe - 25% Cr alloys.

concentration of iron and chromium for the sputter cleaned surfaces of Fe - 13% Cr and Fe - 25% Cr measured as a function of the take-off angle /41/. These results are simply calculated using the sensitivity factors /49/ and the background subtraction /50/. Nevertheless, the concentration of both iron and chromium is clearly found to be independent of the take-off angle, suggesting that the surface composition is quite likely to be the same as that of bulk in the sputtered state. Contrary to this conclusion, it should be kept in mind that measured concentration values by XPS frequently show the take-off angle dependence by inducing surface segregation. Such information will be given later.

3. MODEL FOR DESCRIBING LAYERED STRUCTURE

In order to estimate quantitatively the effective thickness and concentration of surface layers of specimens, the concentration corresponding to a relative XPS signal for constituent elements is discussed here, by coupling with a model as illustrated in Fig.3 (a) and (b) /41/. Although a simple concentration step is assumed in this model, the effective thickness is an indication to express the surface segregated and oxidized layers. The thickness of a single layer with the segregation of an alloying element, t_0, is given in Fig.3(a), and three layers of a contaminated overlayer (thickness, t_1), an alloying element segregated and oxidized layer of (thickness, t_2), and an oxidized layer without segregation (thickness, t_3), are expressed by a model in Fig.3(b). Under a few assumptions such as the absence of elastic scattering and diffraction of photoelectrons, which may be reasonable for polycrystalline specimens, in this three layered structure, the relative intensity, $I_{Xov}(1)$, of specific photoelectrons for element X in the overlayer due to contamination against its bulk /41/ is given by;

$$I_{Xov}(1) = C_{Xov} \times \{ 1-\exp(-t_1/\lambda_{Xov}\sin\theta) \} \quad (1)$$

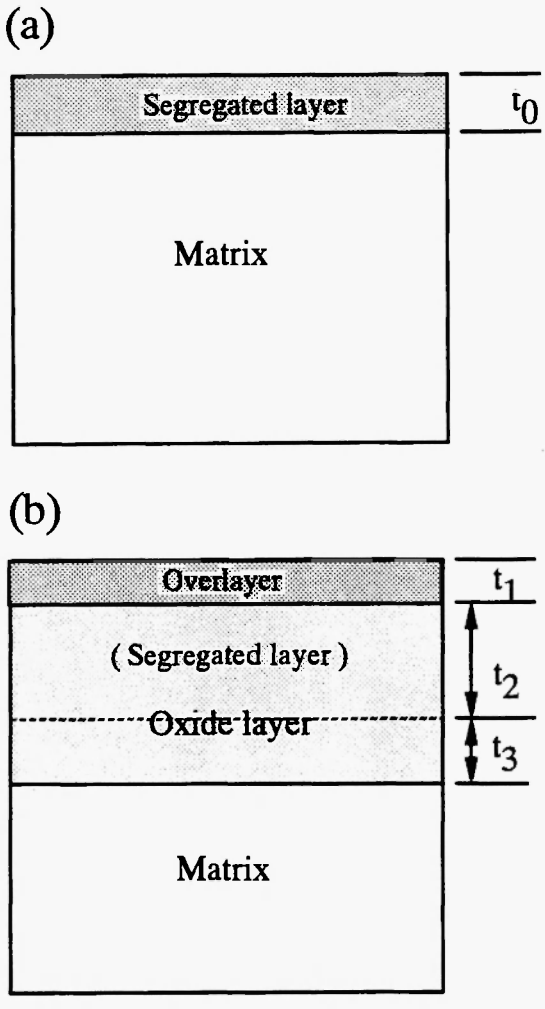

Fig.3: Schematic diagram for layered structures of (a) a segregated layer, (b) an oxide layer formed on the matrix and (c) an oxide layer formed on the segregated surface.

where C_{Xov} and λ_{Xov} are the atomic fraction of element X and the inelastic mean free path of the photoelectron for element X in the overlayer, respectively. θ is the take-off angle.

For the second oxide layer which was taken as an alloying elements segregated and oxidized layer, similar expression can readily be obtained, by taking into account the intensity attenuation of photoelectrons due to the overlayer. The relative intensity, I_{Xox}, for element X ejected from the second layer, may be expressed by;

$$I_{Xox}(2) = C_{Xox}(2)\times\exp(-t_1/\lambda_{Xov}\sin\theta) \times \{ 1 - \exp(-t_2/\lambda_{Xov} \sin\theta) \} \quad (2)$$

where $C_{Xox}(2)$ is the concentration of element X in the oxide layer. λ_{Xov} andλ_{Xov} are the inelastic mean free paths of the photoelectron for element X in the overlayer and in the oxide layer, respectively. For the third layer without the alloying element segregation, its intensity, $I_{Xox}(3)$, can be expressed in a similar way.

In describing the intensities of photoelectrons emitted from the matrix, the influence of the above three layers should be considered. The intensities of photoelectrons for element X emitted from the matrix may, I_{XM}, be given by the following form:

$$I_{XM} = C_{XM} \times \exp(-t_1/\lambda_{Xov}\sin\theta) \times \exp(-t_2/\lambda_{Xov}\sin\theta) \times \exp(-t_3/\lambda_{Xov}\sin\theta) \quad (3)$$

where C_{XM} is the concentration of element X in the matrix.

Although these equations have been applied to characterize a chemically different layer on a substrate /36-38/, it is not unrealistic to extend this idea to intensities of photoelectrons for all kinds of elements. The concentration of element X, C_X, at the take-off angle can be estimated from measured AR-XPS intensity data when coupled with equations (1) to (3), as follows:

$$C_X = [I_{Xov}(1) + I_{Xox}(2) + I_{Xox}(3) + I_{XM}] / IT, \quad (4)$$

where $I_T = \Sigma I_i$.

By fitting equation (4) to the relationship between the concentration and take-off angle for each element, the effective thickness of the overlayer and oxide layer can be estimated when the values of the inelastic mean free paths are given /51,52/.

4. SURFACE SEGREGATION

4.1. Segregation of metallic elements

AR-XPS results on surface segregation of metallic elements such as chromium, nickel, copper, molybdenum, which are important alloying elements in steel, are summarized below. The effective thickness and concentration of surface segregated layers are compared between the alloying elements.

By heating the Fe-Cr specimens at high temperatures under ultra high vacuum, the relative intensity of Cr 2p XPS spectra is increased, while the shape of Fe 2p and Cr 2p XPS spectra shape is unchanged. Figures 4 (a) and (b) show take-off angle dependence of the

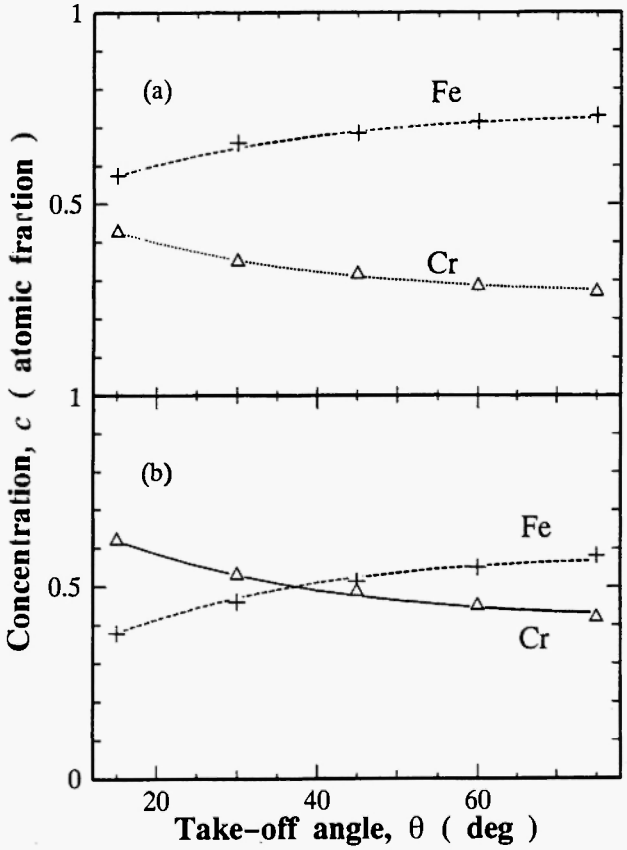

Fig.4: The concentration of iron and chromium versus take-off angle for the chromium surface segregated (a) Fe - 13% Cr and (b) Fe - 25% Cr alloys.

concentration of iron and chromium in Fe - 13%Cr and Fe - 25%Cr heated at 973 K /41/. The concentration was estimated from measured AR-XPS intensity data coupled with the sensitivity of factors of each element, and the experimental results are denoted by marks. The monotonic decrease in the concentration of chromium with increasing take-off angle is found, indicating that chromium is concentrated into the surface region by heating.

Based on the model of the surface segregation as shown in Fig.3(a), the calculated concentrations for chromium and iron are plotted as lines as shown in Fig.4(a) and (b). This good fit enables us to provide the effective thickness and the concentration of the segregated layer, as listed in Table 1, together with other results. It could be suggested that the effective thickness

Table 1
Thickness of segregated layer, t_0, the concentration of an alloying element M in the layer, C_M, formed on the Fe-M alloy surface (see Fig.3).

Specimen (mass%)	t_0 (nm)	C_X (at%)
Fe-13%Cr	0.80	45 %Cr
Fe-25%Cr	0.65	69 %Cr
Fe-0.8%Cu (1073K)	0.4	32 %Cu
Fe-0.8%Cu (873K)	0.5	60 %Cu
Fe-17%Cr-11%Ni-1%Mo-0.08%N	0.8	52%Cr, 6%Ni, 1%Mo, 14%N
Fe-17%Cr-12%Ni-2%Mo-0.08%N	0.8	49%Cr, 6%Ni, 2%Mo, 14%N
Fe-17%Cr-13%Ni-3%Mo-0.07%N	0.8	46%Cr, 7%Ni, 3%Mo, 14%N
Fe-18%Cr-16%Ni-0.06%N	0.8	50%Cr, 11%Ni, 10%N
Fe-18%Cr-16%Ni-0.08%P	0.3(1^{st} layer) 0.5(2^{nd} layer)	35%Cr, 11%Ni, 30%P, 40%Cr, 11%Ni
Fe-18%Cr-16%Ni-0.0007%S	0.3(1^{st} layer) 0.5(2^{nd} layer)	30%Cr, 11%Ni, 30%S 30%Cr, 11%Ni

of the segregated layer does not exceed 1 nm, and the surface segregated amount of chromium is a few times as much as the bulk concentration. The results may indicates that the enriched chromium atoms may actually distribute within not one atomic layer (ca. 0.25 nm) but a few atomic layers.

On the other hand, copper has been found to be considerably segregated to the iron surface in spite of the low bulk concentration /43/. Figure 5 shows the concentration of iron and copper in specimens heated at 873 K and 1073 K as a function of the take-off angle /43/. This take-off angle dependence of the copper concentration is stronger than that for the Fe-Cr system, suggesting that copper is concentrated into a thin surface region. The surface concentration decreases with increasing the heating temperature, although the results at 873 K may include an influence of copper precipitation. Based on the above model for describing

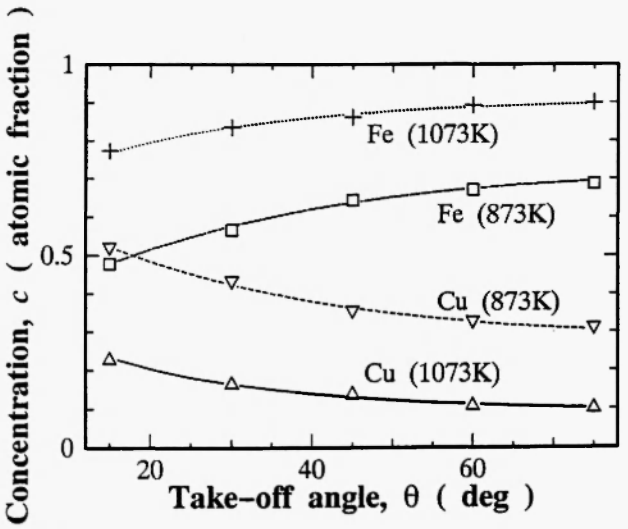

Fig.5: The concentration of iron and copper versus take-off angle for the copper surface segregated Fe – 0.8%Cu alloys by heating at 873K and 1073 K..

surface segregation, the calculated concentrations for copper and iron are plotted as lines, as shown in Fig.5. The effective thickness and the concentration of the segregated layer are listed in Table 1. These results clearly suggest that the surface segregation of copper occurs within a region of nearly single atomic layer on the surface, and the degree of enrichment of copper on the surface to the bulk is considerably high. These results contrast to chromium surface segregation in the Fe-Cr system.

Other metallic elements, such as nickel and molybdenum, have been investigated in multi-components systems based on the Fe-Cr alloy system /42,44/. Table 1 includes the results, which indicates that nickel is likely to be depleted in a surface layer on iron base alloys, whereas molybdenum is slightly segregated to the iron surface by heating under ultra high vacuum. Thus, AR-XPS enables us to provide different characteristic features of surface segregated layers between metallic elements.

4.2. Segregation of non-metallic elements

AR-XPS has been also used for analyzing the effect of non-metallic elements such as nitrogen, phosphorus and sulfur on thin segregated layers formed on the surface of the these high-purity austenitic 18%Cr - 16%Ni steels /44/ and commercial purity austenitic 17%Cr - 12%Ni steels /42/. Since most of the alloying and impurity elements are dissolved in these steels, equilibrium surface segregation of the elements may be measured without influence of formation of a second phase.

Figure 6 shows the variation of take-off angle as a function of the concentration for iron, chromium, nickel, nitrogen, phosphorus and sulfur in Fe - 18%Cr - 16%Ni with (a) 0.06mass%N, (b) 0.08mass%P and (c) 0.007%S, which were heated at 973 K, respectively /44/. The decrease in concentration of nitrogen, phosphorus, sulfur and chromium with increasing take-off angle indicates that these non-metallic elements as well as chromium concentrate on a surface layer. It may be stressed that the take-off angle dependence of the concentration of phosphorus and sulfur is larger than those for chromium and nitrogen. This suggests that phosphorus and sulfur are segregated to a top surface layer, relative to chromium and nitrogen. The fit of calculated curves to the experimental results provides the effective thickness and the concentration of the segregated layer, as summarized in Fig.7 and Table 1. The effective thickness of the segregated layer of chromium is comparable to that for the high-purity iron-chromium steels /41/, and nitrogen seems to be correlated to the chromium segregation. Phosphorus and sulfur are clearly segregated to the top surface. It is

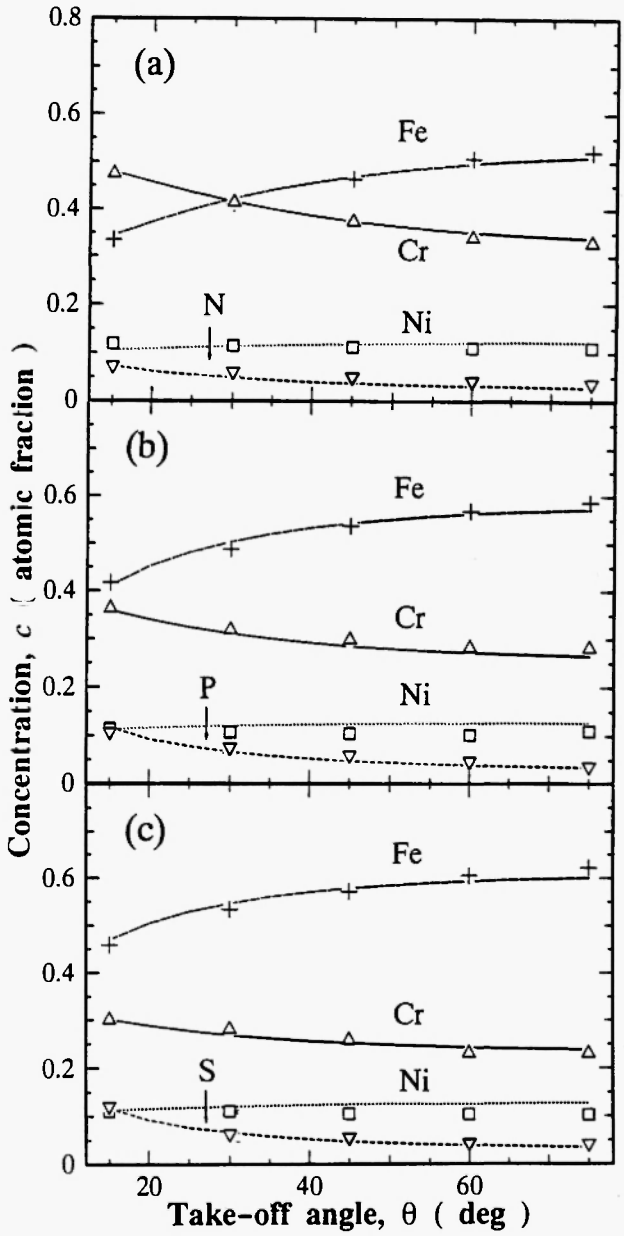

Fig. 6: The concentration of iron, chromium, nitrogen, phosphorus and sulfur versus take-off angle for Fe - 18% Cr – 16%Ni specimens with (a) nitrogen, (b) phosphorus and (c) sulfur.

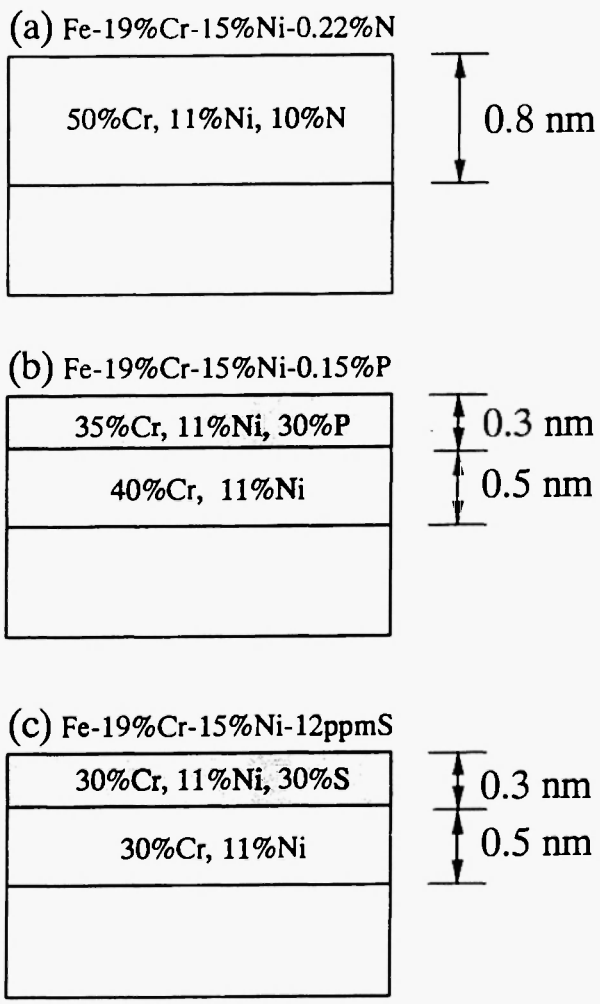

Fig.7: Schematic diagram for layered structures of a surface segregated layer of Fe - 18% Cr - 16%Ni specimens with (a) nitrogen, (b) phosphorus and (c) sulfur. Thickness of segregated layer formed on the surface and the effective concentration (in at% or atppm) are denoted in the figures.

interesting to note in Fig.7 that the degree of chromium segregation is strongly affected by surface segregation of phosphorus and sulfur. This may be attributed to the replacement of chromium with phosphorus or sulfur in the surface layer; that is referred to as site competition on the specimen surface. It is also suggested in Fig.7 that a segregated layer of phosphorus or sulfur is thinner than that of chromium, and they are considered more surface-active than chromium. Thus, the decrease in chromium concentration detected in Figs.6 (b) and (c), as compared to the result of Fig.6(a), may take place through these surface-active behaviors of sulfur and phosphorus. These results may include the effect of different surface orientation in polycrystalline specimens on the surface segregated layers. However, it may be safely said that the present semi-quantitative estimation of the effective thickness and concentration is fairly acceptable, for expressing characteristic features of the surface behaviors of these elements.

5. NATIVE OXIDE LAYER

Native oxide layers are easily formed on the metallic surface only by exposing to air. The native oxide layers are very thin, and its growth process and the effect of the surface composition on the native oxide have also been investigated by AR-XPS. Typical results are given below.

5.1 Native oxide in ultra high-purity iron

Figure 8 shows take-off angle dependence of the measured concentration of iron, copper, oxygen and carbon estimated from measured AR-XPS intensity data for an ultra high-purity iron and copper specimens exposed to air for 1.8×10^3 s, respectively /45/. The experimental values denoted by marks are plotted together with the calculated concentrations (lines) from the model of layered structure, for carbon, oxygen, iron and copper, as shown in Fig.8. In both cases, the monotonic decrease in the concentration of carbon with increasing take-off angle, which is similar to the behavior in surface segregation, suggests that a contaminated layer of hydrocarbon covers the specimens. It is cited in Fig.8 that take-off angle dependence of the oxygen concentration indicates an oxide layer between the overlayer and the matrix. The increase in the measured concentration of iron and copper with increasing take-off angle may result from the reduction of signals of iron by formation of these layers. While the measured copper concentration is dominant in the copper specimen exposed to air for 1.8×10^3 s irrespective of take-off angle, the measured iron concentration is already considerably low in the iron specimen exposed to air. Furthermore, characteristic difference of the concentration by air exposure

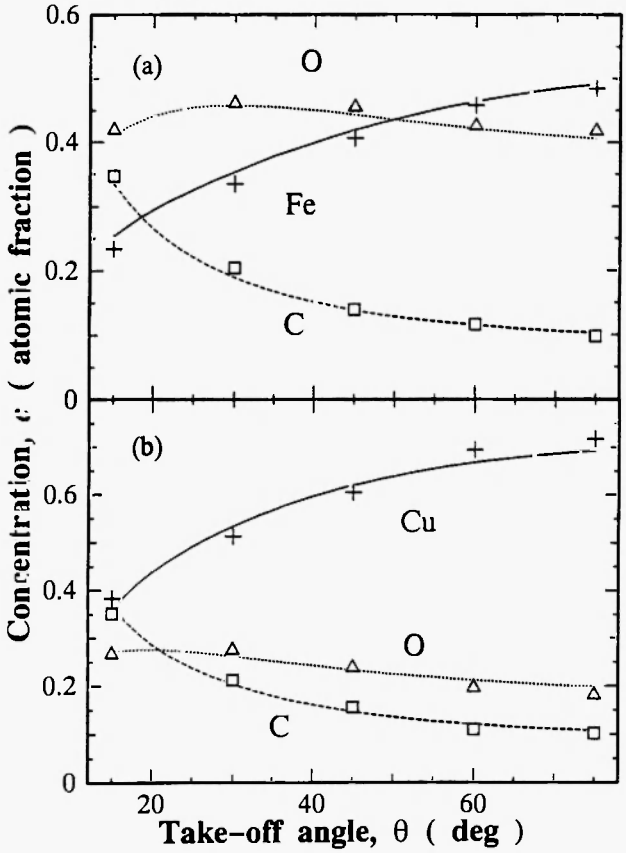

Fig.8: The concentration of iron, oxygen and carbon versus the take-off angle in ultra high-purity (a) iron and (b) copper which are exposed to air for 1.8×10^3s. Experimental and calculated results are denoted by marks and lines, respectively.

time between iron and copper is observed. Figure 9 shows the thickness values of oxide layers and contaminated layers, which were obtained in fitting the calculated results to the experimental ones, as a function of exposure time. The layered structure in this model corresponds to a case without surface segregation of an alloying element as shown in Fig.3(b). The oxide layer thickness for ultra high-purity iron is found to be almost unchanged by exposure time, whereas the oxide layer in ultra high-purity copper becomes considerably thicker in the present exposure condition. These results are consistent with the fact that spectral changes in XPS by air exposure are remarkable in ultra high-purity copper /45/. In addition, the thickness of contaminated layers increases with increasing exposure time in both ultra high-purity iron and copper. The thickness values of

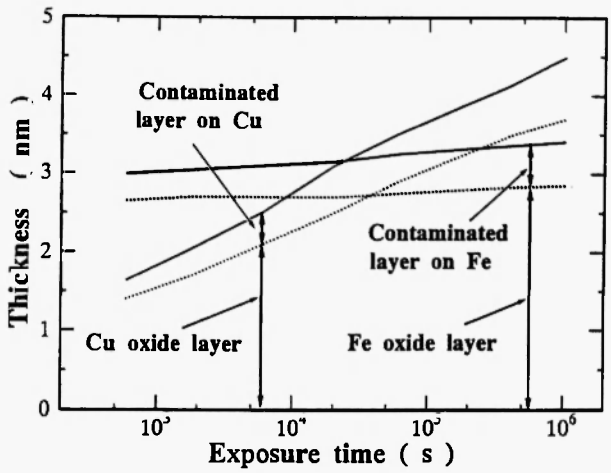

Fig.9: Thickness of oxide layer and contaminated layer formed on the surface of ultra high-purity iron and copper a function of air exposure time.

contaminated layers for ultra high-purity iron and copper appear to be almost independent of species of the substrate, although there is a difference in detail. Thus, there is an advantage in AR-XPS that alternative non-destructive analysis and surface treatment can be done for one specimen, and therefore sequential changes in the specimen surface are feasible.

5.2. Native oxide in Fe-Cr system

Addition of chromium to iron and steel is well-known to be effective in preventing their oxidation, but obvious evidence has not been available from a thin oxide layer formed on the specimen surface at room temperature. AR-XPS is convenient for providing systematic information on the effect of bulk chromium and surface segregated chromium on native oxide layers formed on iron alloys.

As exemplified by the effect of the surface segregated chromium on oxide layers, Figs. 10(a) and (b) show the concentration of iron, chromium, oxygen and carbon estimated from measured AR-XPS intensity data for Fe - 13%Cr and Fe - 25%Cr with chromium segregation as a function of take-off angle, respectively /41/. The specimens were oxidized by air exposure at room temperature for 600 s. Thickness values of these oxide layers can be estimated from the fit of the calculated results to the experimental data, based on the model as shown in Fig.3(b). Figure 11 summarizes the

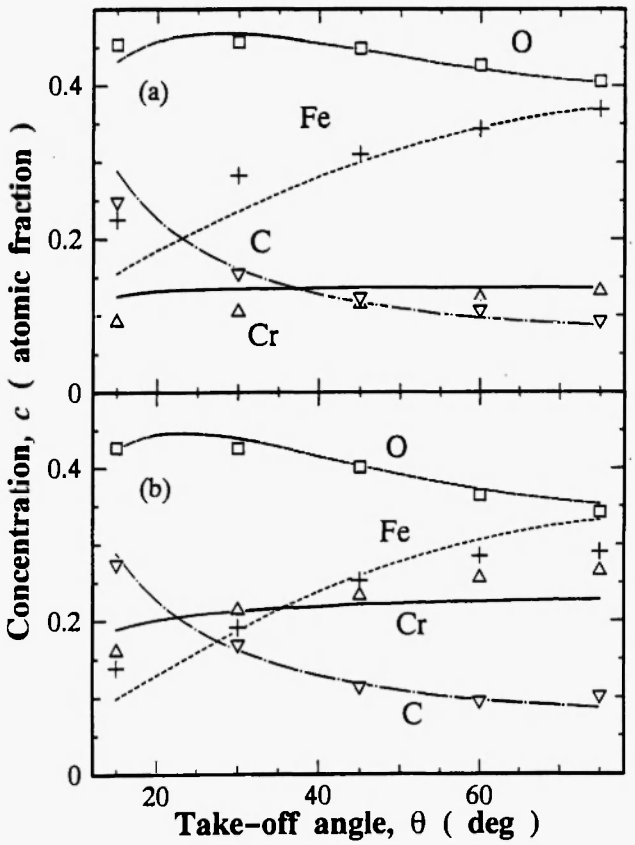

Fig.10: The concentration of iron and chromium versus the take-off angle in (a) Fe - 13 % Cr and (b) Fe - 25 % Cr with chromium segregation which were exposed to air. Experimental and calculated results are denoted by marks and lines, respectively.

thickness of oxide layers formed on the iron-chromium alloys surface versus the bulk chromium concentration. All specimens were oxidized by air exposure at room temperature for 600 s. When the surface concentration is the same as that in the bulk, no surface segregation of chromium is detected. The thickness of oxide layer decreases with increasing concentration of the bulk chromium. In addition, even if the bulk chromium concentration is low, enrichment of chromium by surface segregation appears to induce a decrease in thickness of the oxide layer /41/. More effective reduction of the native oxide formation is found in Fe-Cr-Ni-Mo-N systems /42,44/. This may result from the mutual segregation of chromium and nitrogen on the surface.

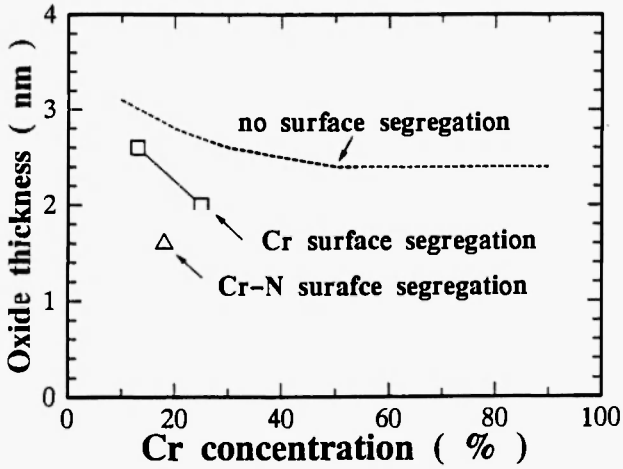

Fig.11: Oxide thickness formed on the surface as a function of the bulk chromium concentration in the iron-chromium alloys.

The effect of chromium surface segregation on reduction in thickness of the native oxide layers is also observed in the XPS spectra. Figures 12 and 13 show AR-XPS spectra of Fe 2p for Fe-17%Cr-12% Ni-2%Mo-0.08%N alloy exposed to air after ion sputtering and the identical alloy exposed to air after surface segregation, respectively. They were obtained in the take-off angle from 15 deg to 75 deg by a step of 15 deg. For comparison, Figure 12(f) indicates the XPS spectrum of Fe 2p from the virgin surface as cleaned by ion sputtering, which correspond to the metallic surface. The spectra of Fe 2p for the specimens exposed to air can be allocated to the signals from Fe^0 (Fe $2p_{3/2}$: 707 eV) and Fe oxide (Fe^{2+} (Fe $2p_{3/2}$: 710 eV) and Fe^{3+} (Fe $2p_{3/2}$: 711 eV). The valence number of the oxides formed may be mainly assigned to 3+. It may also be stressed in these figures that the relative intensities of metallic peaks to oxide peaks in the Fe 2p spectra increase with take-off angle. Since XPS signals measured at higher take-off angles are known to arise mainly from a deep part of the specimens, these results indicate that the matrix of specimens is considered metallic and the thickness of oxide layer formed on the surface are comparable to the mean free path of photoelectrons.

It is clearly shown in Figs.12 and 13 that the surface segregation of chromium and additionally nitrogen reduces the thickness of the oxide layers. In order to

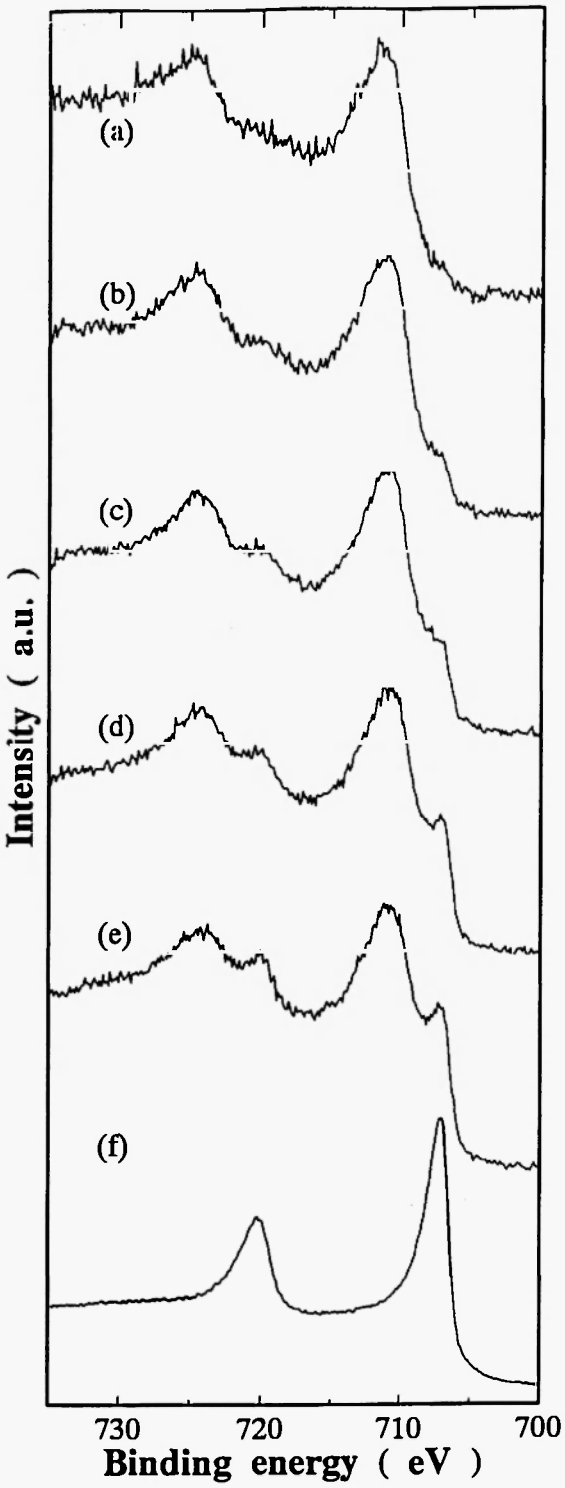

Fig.12: Fe 2p AR-XPS spectra obtained in the take-off angle of (a) 15 deg, (b) 30 deg , (c) 45 deg, (d) 60 deg and (e) 75 deg for Fe - 18% Cr –12%Ni - N exposed to air after sputtering. (f) Fe 2p XPS spectrum in a sputter cleaned surface.

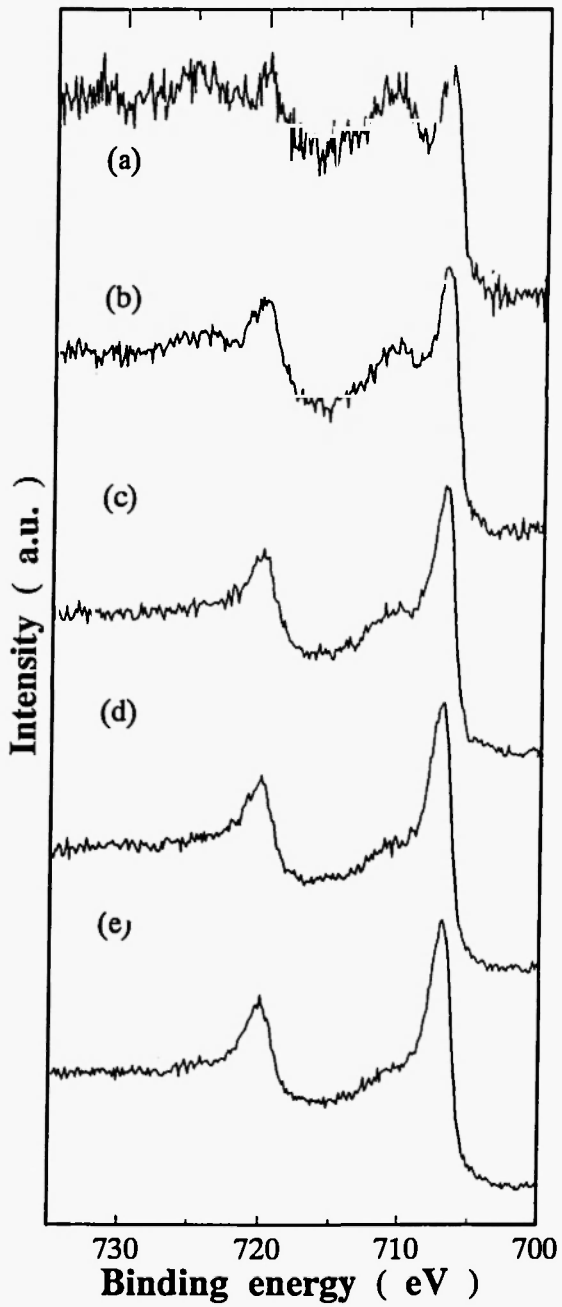

Fig.13: Fe 2p AR-XPS spectra obtained in the take-off angle of (a) 15 deg, (b) 30 deg , (c) 45 deg, (d) 60 deg and (e) 75 deg for Fe - 18% Cr –12%Ni - N exposed to air after surface segregation.

examine the relationship between the surface segregation and the oxidation, peak height ratios metallic peak to oxide peak in Fe $2p_{3/2}$ of oxide peak to metallic peak are plotted as a function of the maximum concentration of chromium in the surface layer before

air exposure in Fe-Cr alloys as shown in Fig.14. A positive correlation is found in this plot, with a few exceptions showing very strong effect of surface segregation for specimens with higher nitrogen and molybdenum. Thus, it is suggested that the surface properties of iron-chromium alloys can be controlled by changing the surface concentration near the surface region, and for such purpose, it would be encouraging to modify the process conditions for the sample surface such as atmosphere and annealing temperature.

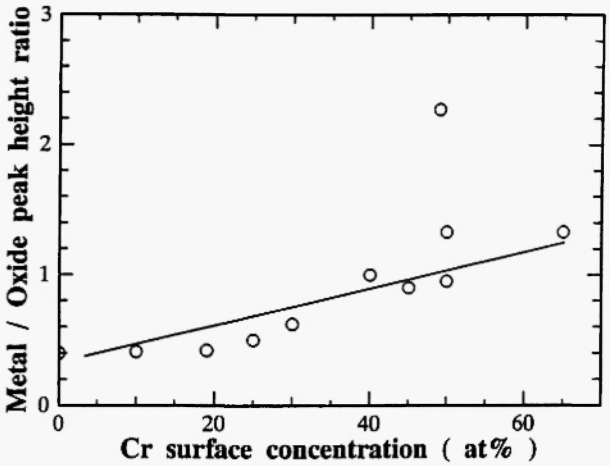

Fig.14: Plot between the peak height ratio of metallic peak to oxide peak in Fe $2p_{3/2}$ of Fe-Cr specimens exposed to air and the maximum chromium concentration in surface layers before air exposure.

6. SUMMARY

AR-XPS has been systematically used for investigating surface segregation of alloying and impurity elements in high-purity base iron alloys. It was also applied to characterize oxide layers formed on the surface of those alloys at room temperature. The main results are summarized as follows:

(1) Metallic elements such as chromium and copper were clearly segregated to the iron surface by *in-situ* heating at about 1000 K under ultra high vacuum (10^{-8}Pa). The effective thickness of segregated layers is estimated to be less than 1 nm, although it depends upon segregated element. The degree of enrichment of copper in the segregated layer to the bulk concentration is higher than that for chromium. Nickel is likely to be depleted in the surface layer, whereas molybdenum is slightly segregated.

(2) Non-metallic elements such as nitrogen, phosphorus and sulfur are easily segregated to the iron surface. While nitrogen is mutually segregated with chromium in the surface layer, phosphorus and sulfur appear to replace chromium segregation.

(3) The surface segregation of chromium reduces the thickens of the native oxide layer formed on iron-chromium alloys, although the segregated layer is thinner than the oxide layer. The results on the layered structure obtained from the take-off angle dependence of the concentration are consistent with information on the chemical state of Fe 2p.

ACKNOWLEDGEMENTS

The author expresses deep thanks to Prof.Y.Waseda, Prof.M.Isshiki and Prof.M.Tanino for their continuous support and encouragement.

REFERENCES

1. H.J. Grabke, G. Tauber and H. Viefhaus, *Scripta Metall.*, 9, 1181 (1975).
2. H.J. Grabke, W. Paulitsche, G. Tauber and H. Viefhaus, *Surf. Sci.*, 3, 377 (1977).
3. H.J. Grabke, H. Viefhaus and G. Tauber, *Arch. Eisenhuttenw.*, 49, 391 (1978).
4. H.J. Grabke, *Mater., Sci. Eng.*, 42, 91 (1980).
5. N. Egert, H.J. Grabke, Y. Sakisaka and T.N. Rhodin, *Surf. Sci.*, 141, 397 (1984).
6. H. de.Rugy and H.J. Grabke, *Surf.Sci.*, 109, 418 (1986).
7. L. Marchut and C.J. McMahon, Jr:, *Metal. Trans.*, 12A,1135 (1981).
8. J. du Plessis and P.E. Viljoen, *Surf. Sci.*, 131, 321 (1983).
9. F. Bezuidenhout, J. du Plessis and P.E. Viljoen, *Surf. Sci.*, 171, 397 (1986).
10. B. Egert and G. Panzner, *Surf.Sci.*, 118, 345

(1985).

11. M.P. Seah and C. Lea, *Phil.Mag.*, **31**, 627 (1975).
12. C. Lea and M.P. Seah, *Phil.Mag.*, **31**, 213 (1977).
13. H. Viefhaus and M. Rusenberg, *Surf.Sci.*, **159**, 1 (1985).
14. Y.X. Zhou, R. Hsiao, C.J. McMahon,Jr. and E.W. Plummer, *Surf.Sci.*, 179, 209 (1987).
15. L. Marchut, T.M. Buck, C.J. McMahon, Jr., G.H. Wheatley and W.M. Augstyniak, *Surf.Sci.*, 180, 252 (1987).
16. L.Q. Clayton and G.T. Burstein, *Met.Sci.*, 13, 530 (1979).
17. M. Oku, K. Hitokawa, H. Kimura and S. Suzuki, *Surf. Interface Anal.*, 8, 67 (1986).
18. M. Rusenberg and H. Viefhaus, *Surf.Sci.*, **172**, 615 (1986).
19. Ph. Doumoulin and H. Guttmann, *Mater.Sci. Eng.*, 42, 249 (1980).
20. C. Leygraf, G. Hultquist, S. Ekelund and J.C. Ericksson, *Surf. Sci.*, 46, 157 (1974).
21. C. Leygraf, G. Hultquist and S. Ekelund, *Surf. Sci.*, **51**, 409 (1975).
22. C. Leygraf and G. Hultquist, *Surf.Sci.*, **61** , 60 (1976).
23. C. Leygraf and G. Hultquist, *Surf.Sci.*, **61**, 69 (1976).
24. W. Yu-Quing and C.J. McMahon, Jr., *Scripta Metall.*, **20**, 19(1986).
25. C.L. Briant, *Surf.Interface Anal.*, **13**, 209 (1988).
26. C. Uebing, H. Viefhaus and H.J. Grabke, *Appl. Surf. Sci.*, **32**, 363 (1988).
27. H.J. Grabke, *Surf. Interface Anal.*, 14, 209 (1989).
28. C. Uebing, *Surf. Sci.*, **225**, 97 (1990).
29. S. Suzuki, *Mater. Trans. JIM*, **31**, 1085 (1990).
30. I. Olefjord, *Corros.Sci.*, **15**, 687 (1975).
31. G. Hultquist and C. Leygraf, *Corros.Sci.*, **22**, 331 (1982).
32. T.G. Hultquist, M. Seo and N. Sato, *Oxid. Metals*, 25,363 (1986).
33. H.J. Mathieu and D. Landolt, *Appl. Surf. Sci.*, **3**, 348 (1979).
34. J.E. Castle, R. Ke and J.F. Watts, *Corros. Sci.*, **30**, 771 (1990).
35. H.J. Mathieu and D. Landolt, *Surf. Interface Anal.*, 14, 744 (1989).
36. C. Palcio,H.J. Mathieu and D .Landolt, *Surf. Sci.*, 214, 493 (1989).
37. C. Palcio, H.J. Mathieu, V. Stambouli and D. Landolt, *Surf. Sci.*, **295**, 547 (1993).
38. J.M. Hill, D.G. Royce, C.S. Fadley, L.F. Wagner and F.J. Grunthaner, *Chem. Phys. Lett.*, 44, 225 (1976).
39. S. Suzuki,T. Kosaka,H. Inoue and Y. Waseda, *Materials Trans.JIM*, **36**, 1379 (1995).
40. S. Suzuki,T. Kosaka,H. Inoue and Y. Waseda, *Iron Steel Inst. Japan*, **36**,433 (1996).
41. S. Suzuki,T. Kosaka,H. Inoue, M. Isshiki and Y. Waseda, *Appl.Surf.Sci.*, **103**, 495 (1996).
42. S. Suzuki, T. Nakazawa and Y. Waseda, *Iron Steel Inst. Japan*, **36**, 1273 (1996).
43. S. Suzuki and Y. Waseda, *Scripta Mater.*, **36**, 915 (1997).
44. S. Suzuki, U. Tsu, T. Ohtsuka, T. Shindo, M. Tanino and Y. Waseda, *ECASIA '97*, John Wiley (1997), in press.
45. S. Suzuki, Y. Ishikawa, M. Isshiki and Y. Waseda, *submitted to Materials Trans.JIM.*
46. K. Sugimoto, S. Matsuda, M. Isshiki, T. Ejima and K. Igaki, *J.Japan Inst. Metals*, **46** , 155 (1982).
47. K. Sugimoto, N. Hara, M. Isshiki, T. Ejima and K. Igaki, *J.Japan Inst. Metals*, 46, 703 (1982).
48. D. McLean, *Grain Boundaries in Metals*, Oxford University Press, London, (1957), p.116.
49. J.F. Moudler, W.F. Sticle, P.E. Sobol and K. Bomben, *X-ray photoelectron spectroscopy*, Physcal Electronics, Minnesota, (1993), p.219.
50. D.A. Shirley, *Phys. Rev.*, **B5**, 4709 (1972).
51. S. Tanuma, C.J. Powell and D.R. Penn, *Surf. Interface Anal.*, **11**, 577 (1988).
52. S. Tanuma, C.J. Powell and D.R. Penn, *Surf. Interface Anal.*, 17, 911 (1991).